Eur Biophys J (1986) 13:259–271

European Biophysics Journal

Sodium channels in cultured chick dorsal root ganglion neurons

E. Carbone* and H. D. Lux

Max-Planck-Institut für Psychiatrie, Abteilung Neurophysiologie, Am Klopferspitz 18A, D-8033 Planegg, Federal Republic of Germany

Received June 17, 1985/Accepted October 15, 1985

Abstract. Isolated Na currents were studied in cultured chick sensory neurons using the patch clamp technique. On membrane depolarization, whole cell currents showed the typical transient and voltage-dependent time course as in nerve fibres. Na currents appeared at about − 40 mV and reached maximum amplitude at around − 10 mV. At low voltages (− 30 to 0 mV), their turning-on was sigmoidal and inactivation developed exponentially. The ratio of inactivation time constants was found to be smaller than in squid axons and comparable to that of mammalian nodes of Ranvier. Peak conductance and steady-state inactivation were strongly voltage-dependent, with maximum slopes at − 17 and − 40 mV, respectively. The reversal potential was close to the Nernst equilibrium potential, indicating a high degree of ion-selectivity for the channel. Addition of 3 μ*M* TTX, or replacement of Na by Choline in the external bath, abolished these currents. Internal pronase (1 mg/ml) and N-bromoacetamide (0.4 m*M*) made inactivation incomplete, with little effect on its rate of decay.

Single Na channel currents were studied in outside-out membrane patches, at potentials between − 50 and − 20 mV. Their activation required large negative holding potentials (< − 90 mV). They were fully blocked by addition of TTX (3 μ*M*) to the external bath. At − 40 mV their mean open time was about 2 ms and the amplitude distribution could be fitted by a single Gaussian curve, indicating the presence of a homogeneous population of channels with a conductance of 11 ± 2 pS. Probability of opening increased and latency to first opening decreased with increasing depolarization. Inactivation of the channel became faster with stronger depolarizations, as measured from the inactivation time course of sample averages. Internal pronase (0.1 mg/ml) produced effects on inactivation comparable to those on whole cell currents. Openings of the channel had a tendency to occur in bursts and showed little inactivation during pulses of 250 ms duration. The open lifetime of the channel at low potentials (− 50, − 40 mV) was only three times larger than in control patches, suggesting that Na channels in chick sensory neurons can close several times before entering an inactivating absorbing state.

Key words: Sodium channels, patch-clamp, sensory neurons

Introduction

Action potentials at the cell body of vertebrate dorsal root ganglion (DRG) neurons originate from transient increases of membrane permeability to Na^+ and Ca^{2+} ions (Dichter and Fischbach 1977; Baccaglini 1978). Ca^{2+} currents are of considerable size in DRG cells and have been investigated in detail (Dunlap and Fischbach 1981; Kostyuk et al. 1981; Kameyama 1983; Ishizuka et al. 1984). Recently, it was shown that they could be separated into two components with different kinetics, voltage-dependency and single channel properties (Carbone and Lux 1984a, b). Also, two Na currents were identified in rat DRG (Kostyuk et al. 1981). A TTX-sensitive component resembles the fast Na current responsible for the rising phase of the action potential of nerve fibres (Hodgkin and Huxley 1952b). The other one, TTX-resistant, shows slower activation-inactivation kinetics and is blocked by nominal Ca channel blockers. There are no reports of unitary Na currents in DRG cells despite the need for a better understanding of the excitation process of vertebrate sensory neurons.

* *Offprint requests to:* E. Carbone, Istituto di Cibernetica e Biofisica del C.N.R., Corso Mazzini 20, I-16032 Camogli, Italy

In the present paper, we have analyzed the properties of whole cell and unitary Na currents in primary cultures of chick DRG cells, using the patch clamp technique (Hamill et al. 1981). Our results suggest that Na currents in these cells are delivered from a homogeneous population of TTX-sensitive Na channels with kinetics, single channel conductance, and pharmacological properties similar to the Na channels of other excitable cells (Sigworth and Neher 1980; Fenwick et al. 1982; Nagy et al. 1983; Cachelin et al. 1983; Fernandez et al. 1984). They can be recorded at various stages of cell growth from embryos after the tenth day of development. Their density is one to two orders of magnitude smaller, and inactivation is faster than in peripheral nerve fibers (Hodgkin and Huxley 1952b; Conti et al. 1975). This could be of relevance for the firing behavior of DRG cells. No evidence has been found for the existence of TTX-resistant Na channels in this preparation.

The close similarity of the activation-inactivation kinetics with other Na currents (Moolenar and Spector 1978; Matteson and Armstrong 1983) also allows some consideration of recent models of Na inactivation drawn from single channel analysis (Aldrich et al. 1983; Horn et al. 1984; Horn and Vandenberg 1984).

A preliminary account of this work has already appeared (Carbone and Lux 1984c).

Materials and methods

The experiments were performed on primary cultures of dorsal root ganglia of *Gallus domesticus*. Sensory neurons from the lumbar region were dissociated from 10 day old embryos and grown in a 35 mm plastic petri dish following the procedure of Barde et al. (1980). Special care was taken to separate the dorsal root from sympathetic ganglia. Whole-cell and out-side-out membrane patches were made according to the method of Hamill et al. (1981). The experimental set-up, fabrication of patch electrodes, and I-V converter were similar to those described elsewhere (Lux and Brown 1984; Carbone and Lux 1984a).

Solutions

The compositions of the solutions used are listed in Table 1. Solutions were buffered to pH 7.3 ± 0.1 and filtered through 0.2 µm Millipore filters before use. To improve the quality of the patch conditions, the osmolarity of the pipette-filling solution was maintained at 20% below that of the external medium. To remove steady-state Na inactivation, 0.4 m*M* N-bromoacetamide (Sigma Chemical Co., St. Louis, MO) or 1 mg/ml pronase E (Merck, Darmstadt, FRG) was added to the filling solution of the patch pipettes.

Whole-cell currents recording

Membrane current records were stored on an FM tape recorder at 5 kHz bandwidth. Data were digitized at sampling rates of 70 to 150 µs using a 12-bit analog-to-digital converter in combination with an LSI 11/23 minicomputer. Leakage and capacitative current components were reduced by analogue compensation circuitry and the residual minimized by subtracting appropriately scaled currents from inverted pulse paradigms. To improve the response of the patch clamp system, the electrode series resistance was partially compensated by positive feedback. Using electrodes of about 3 M Ω resistance and cells of 10 µm diameter, the response time constant was between 70 and 150 µs before series resistance compensation, this was reduced to nearly half after compensation. Care was taken to record from cells in which inward and outward membrane currents did not exceed 1 nA, to be well below feedback saturation. This also limited the errors introduced by an uncompensated series resistance to 1 to 5 mV. The resolution of the time course of membrane currents was improved by lowering the bath temperature to 12 ± 0.3 °C by means of a Peltier system with a thermistor in the feedback loop. Data were not corrected for liquid-junction potentials.

At rest, cells were held at a potential varying between -70 and -80 mV (E_h). Depolarizations to test levels (E_t) lasted for 20 to 100 ms and were applied at intervals of 3 to 5 s. Steady-state inactivation (h_∞) was determined by the two-pulse procedure (Hodgkin and Huxley 1952a). The conditioning prepulses lasted for 50 ms and varied from -110 mV to -10 mV. Test potential was 0 or $+10$ mV.

A total of 250 cells of different shapes and sizes were whole cell clamped. However, only about 80 of them were found to fulfill the criteria for reliable recordings, i.e.: *i*) seal resistance > 50 GΩ before and after establishment of whole cell current recording; *ii*) high input membrane resistance at rest (6 to 12 GΩ); *iii*) low series resistance (4 to 6 MΩ), indicating an almost unobstructed access of the electrode to the cell interior after rupture of the cell membrane; *iv*) appropriate voltage- and space-clamp control, evidenced by the absence of "notches" on the current traces at low potentials (-40 to -10 mV); and *v*) reproducible current recording for approxi-

mately 20 min. Such recording conditions were best achieved when freshly prepared cells of 6 to 12 h incubation were used. At this stage of growth, most DRG cells are round (5 to 15 μm in diameter) and have no processes. The rate of success in obtaining seals of high resistance from these cells is very high, and establishment of the whole cell recording very often leads to a complete break through the cell membrane, as evidenced by the large amplitude and small time constant of the decaying part of the capacitive artifact. The kinetic properties of Na channels from these cells were consistently found to be similar to those of mature cells (1 to 4 day incubation) which were larger in size (20 to 40 μm) and possessed long processes. On the other hand, recordings from cells more than one day in culture, normally created space-clamp difficulties, and as such they were discarded.

Occasionally, during experiments lasting 20 to 30 min, a shift of 5 to 10 mV of the current-voltage characteristics was observed, as also described for pituitary cells by Fernandez et al. (1984). To minimize such error, Na currents were routinely recorded 5 to 10 min after establishment of the whole cell patch. In agreement with previous reports (Fenwick et al. 1982; Nagy et al. 1983; Carbone and Lux 1984b) 10 to 15 mV shifts of the Na voltage-dependent parameters were systematically observed between outside-out and whole cell recordings (see Results).

Single channel recording

Unitary Na currents were recorded from excised membrane patches in the outside-out configuration using pipettes of 5 to 10 MΩ resistance (Hamill et al. 1981). At rest, the patch was maintained at potentials between −80 and −100 mV. Test depolarizations of 70 to 300 ms were applied every 2–3 s. Membrane patches lasted 20 to 40 min on the average, with little sign of rundown of channel activity. Usually, the disappearance of channel activity was abrupt and coincided with the deterioration of the patch conditions. The lifetime of the patches was reduced when pronase was added to the pipette-filling solution to remove Na inactivation. Under these conditions, the patches lasted only 5 to 15 min and showed a continuous increase of the steady-state leakage current with time.

To avoid signal saturation of the I-V converter, the capacitive artifact was largely reduced by ON-line analogue compensation. The residual transient component was accurately corrected OFF-line, by subtracting from each single channel recording an appropriately scaled signal which was the average of 30 to 40 traces associated with step depolarizations of low amplitude (20 mV) without channel activity.

Unitary events were analyzed as described elsewhere (Lux and Brown 1984; Carbone and Lux 1984b). The analog data were filtered before digitization using a 4 pole Bessel filter with a corner frequency of 1 or 3 kHz. Digitization was done at rates of 70 μs per point using a maximum of 4,096 points per curve. To obtain amplitude and time histograms, single channel currents were converted into idealized events by means of an interactive computer program. The criteria for selecting the detection level of channel opening and closing as well as the estimate of the number of false events were similar to those previously described (Lux and Brown 1984). The effective minimal duration of detectable openings was set to 140 μs. The number of channels in a patch was estimated from the maximum current amplitude occurring in a large sample of recordings at strong depolarizations (Aldrich et al. 1983). Mean open times in multichannel patches were estimated following the procedure used by Fenwick et al. (1982), and Horn and Lange (1983).

Results

Major ionic currents

Figure 1A shows a family of current records obtained during step depolarizations of a voltage-clamped DRG cell. The external medium contained 120 m*M* Na and 1 m*M* Ca, while the pipette contained 120 m*M* K. At potentials between −36 and −12 mV, membrane currents were predominantly inward. Outward currents appeared at more positive membrane potentials (0 mV) to gain considerable amplitudes at stronger depolarizations. Several lines of evidence indicated that inward currents were carried mainly by Na ions: *i*) activation and inactivation of this component developed in the millisecond time scale; *ii*) the peak amplitude was strongly voltage-dependent in the range −30 to −10 mV (Fig. 1B); *iii*) the reversal potential for this current (+65 mV) was close to that predicted by the Nernst equation (+68 mV) for $Na_o = 120$ m*M* and $Na_i = 8$ m*M*; and *iv*) inward currents were fully blocked after adding 3 μ*M* TTX to the bath and were absent when Na was replaced by choline (see below).

Under normal ionic conditions, outward currents were mainly carried by K ions and could be considerably reduced when the cell was dialyzed with solutions containing Cs und TEA. No attempt was made to study voltage-dependent, Ca^{2+}-dependent and transiently-activated (I_A) K currents in more detail.

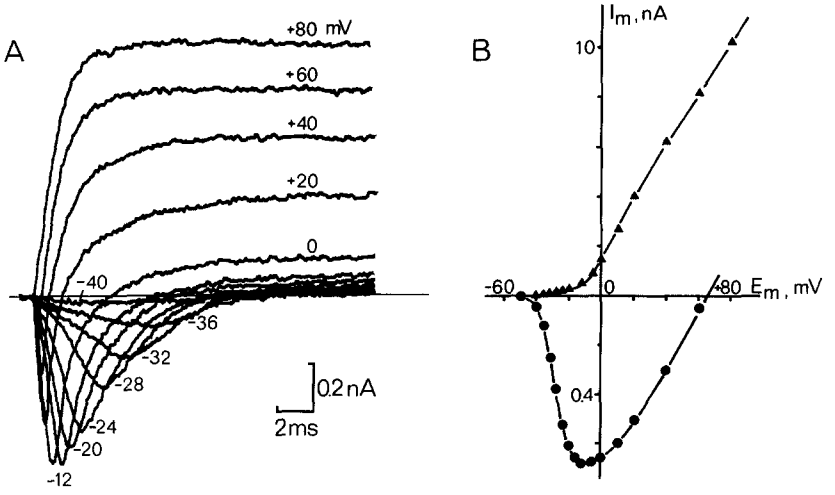

Fig. 1. Whole cell currents in normal internal and external solutions. **A** Time course of major current components recorded from a DRG cell clamped at the potential indicated. **B** Peak *(circles)* and steady-state *(triangles)* I-V relationship of the whole cell currents illustrated in **A**. Inward currents appear to activate at − 40 mV and reverse at about + 70 mV. The holding potential was − 70 mV. *Out:* 120 Na, 1 Ca. *In:* 120 K

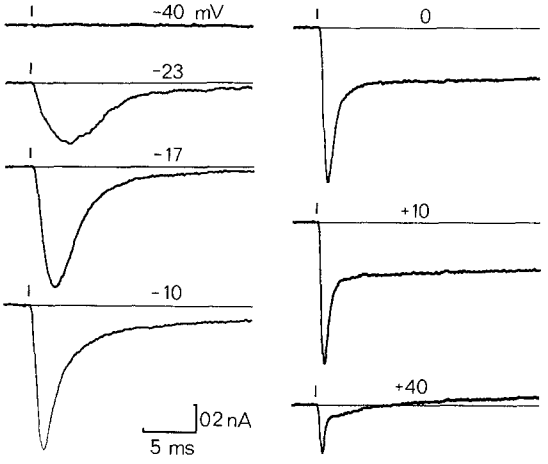

Fig. 2. Time course of inward currents recorded in the presence of internal Cs and TEA at the potential indicated. Bar on each record indicates the onset of step depolarization. Note the small persistent outward current components at + 40 mV. Holding potential: − 70 mV. *Out:* 120 Na, 2 Ca. *In:* 120 Cs

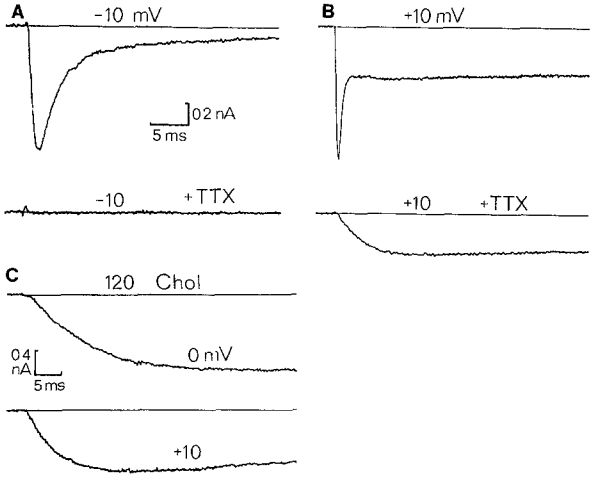

Inward currents in cells perfused with Cs und TEA

Typical inward currents of DRG cells internally perfused with Cs and TEA are illustrated in Fig. 2. A fast transient and a persistent current component could be distinguished. The fast component was present at all potentials investigated (− 40 to + 40 mV). Its time to peak decreased considerably and its inactivation was faster with increasing membrane depolarizations. At − 17 mV this current was fully inactivated at the termination of a 25 ms pulse. The persistent component was more evident at potentials positive to − 10 mV. It reached a maximum amplitude between 0 and + 10 mV and showed very slow time-dependent inactivation.

The fast current component disappeared after addition of 3 μ*M* TTX to the bath (Fig. 3A and B) and was also absent when choline replaced external Na (Fig. 3C). The slow component persisted in the presence of choline and TTX but was sensitive to external Ca. At + 10 mV in 5 m*M* Ca_o (Fig. 4C), this component was nearly twice that recorded in 2 m*M* Ca_o at the same potential (Fig. 3B). This indicated that the fast transient current was carried mainly by Na^+ ions and the maintained current by

Fig. 3A and B. Block of the fast inward current component by TTX. Current traces at − 10 mV (**A**) and + 10 mV (**B**) were recorded before *(top record)* and after *(bottom record)* addition of 3 μ*M* TTX to the external bath. At − 10 mV, the inward current could be fully blocked by TTX, while a slow inward component persisted at + 10 mV. Holding potential: − 70 mV. *Out:* 120 Na, 2 Ca. *In:* 130 Cs. **C)** Time course of the slow persistent inward current component in the presence of 120 m*M* choline. Membrane potentials are indicated on top of each record. Note the larger amplitude of the current record at + 10 mV with respect to that in **B** *(lower record)*. External Ca^{2+} was 5 m*M*. Holding potential: − 70 mV. *Out:* 120 Chol. *In:* 130 Cs

Ca^{2+} (for more details on the Ca current of this preparation see Carbone and Lux 1984a).

In all the cells analyzed, including 40 rat DRG neurons (Carbone and Lux 1984b), we did not observe signs of TTX-resistant Na currents such as those reported in new-born rat DRG cells (Kostyuk et al. 1981). These currents are sensitive to Ca^{2+} channel blockers and have time constants of activation and inactivation about ten times larger than those that are TTX-sensitive. We do not have a clear explanation for such a discrepancy. One possibility is that TTX-resistant currents characterize a small percentage (10 – 15%) of DRG cells which are present in 5- to 10-day-old rats, but not at the embryonic stage. Another possibility is that internal perfusion conditions with fluoride salts, as used in new-born rats, might be crucial for the survival of these currents during whole cell recording. Finally, it is also possible that TTX-resistant Na channels change their properties when cells are grown in short-term cultures.

Separation of Na currents from other membrane currents

Inward Na currents were separated from Ca currents by substituting external Ca^{2+} by Mg^{2+} (Fig. 4), which reversibly suppressed the persistent current component. Other nominal Ca channel blockers such as Ni^{2+}, Cd^{2+} and Co^{2+} yielded the same result. At low voltages (– 30 to – 10 mV), current traces revealed the transient time course typical of Na currents in nerves with a fast sigmoidal rise. Inactivation followed a single exponential decay and was nearly complete after 20 to 30 ms. Times to peak and rates of inactivation were strongly voltage-dependent. The former was reduced about threefold and the latter five times accelerated, upon increasing the step depolarization from – 26 to – 10 mV.

At potentials beyond 0 mV, Na currents (I_{Na}) appeared to be distorted by the presence of additional membrane currents. Figure 4 shows a residual persistent inward current even after 20 ms which could be attributed to: *i*) a maintained Na current (Chandler and Meves 1970a); *ii*) a Ca current component due to Ca^{2+} impurities (1 to 10 μM) in the bath; or *iii*) the passage of Na^+ or Mg^{2+} ions through Ca^{2+} channels (Almers and McClenskey 1984; Hess and Tsien 1984). At higher voltages (above + 20 mV), the peak current was followed in this cell by a sizeable outward component very likely resulting from incomplete block of K^+ channels by internal Cs and TEA. The amplitude of this component increased with voltage and was quite variable from cell to cell. In some cases, in which this component was sufficiently small, the Na equilibrium potential, E_{Na}, could be estimated rather accurately (see inset of Fig. 4). At + 60 mV, peak I_{Na} was still inward despite the presence of a delayed persistent outward current. At + 70 mV, the peak was net outward and appeared to level off before the rise of the outward component. This set E_{Na} to about + 65 mV, which was corroborated by linear-approximation of peak transients over a wider range of voltages. This value was close to that predicted by the Nernst equation (+ 66.3 mV) for the present conditions of 120 mM Na_o and 8 mM Na_i, at 12 °C.

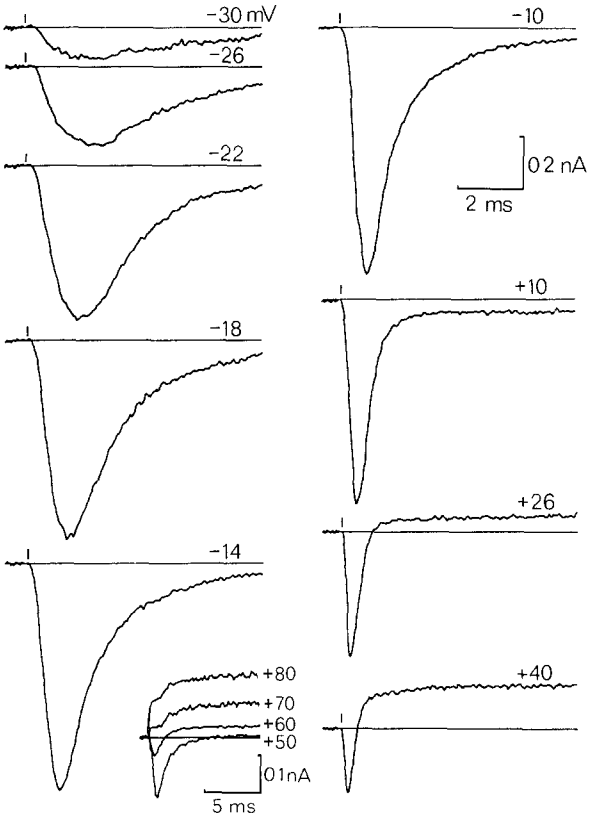

Fig. 4. Time course of Na^+ currents in the absence of external Ca^{2+}, at the potential indicated. External Ca^{2+} was replaced by Mg^{2+}. At + 10 mV, there is a small maintained level of inward current at long times. At + 26 and + 40 mV, a slow outward current is visible after the fast transient Na component. *Inset:* Reversal of Na^+ currents. Current records were obtained from a different cell at large membrane potentials (+ 50 to + 80 mV). Despite the presence of the outward current component, the peak Na current is clearly seen to reverse at about + 65 mV. Holding potential: – 70 mV. *Out:* 120 Na, 7 Mg. *In:* 130 Cs

Na conductance parameters

To determine the time course of Na currents at large depolarizations, a subtraction procedure was used to eliminate the distortions introduced by residual

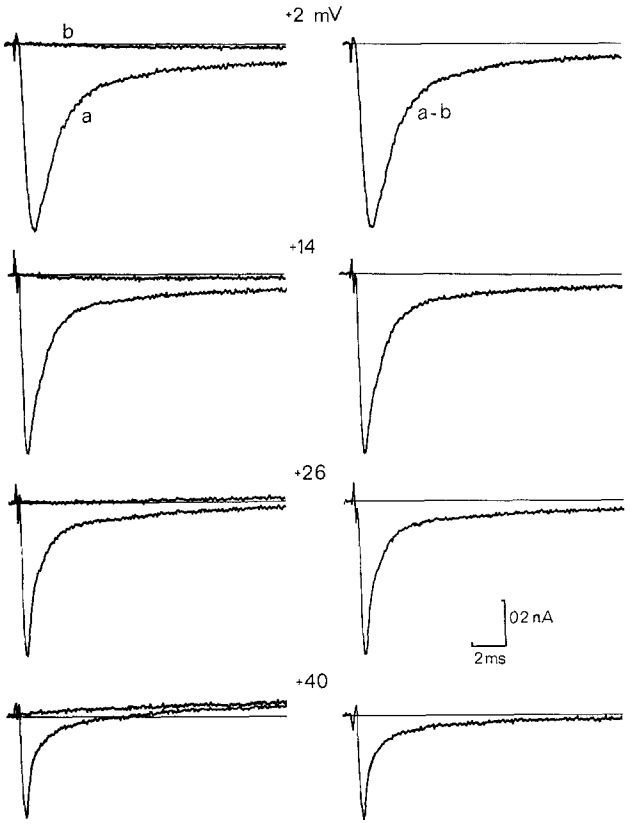

Fig. 5. Time course of I_{Na} after correction for TTX-insensitive currents. Na^+ currents were recorded under the conditions of Fig. 4, before (trace *a*) and after (trace *b*) the addition of 3 μM TTX at the potentials indicated. Trace ($a-b$) is the computed difference of records (*a*) and (*b*). By definition, traces of the type (*b*) are indicated as TTX-insensitive currents (Meves 1978). At + 2 and + 14 mV, TTX-insensitive components are inward and contribute very little to the total current. At potentials above + 26 mV, they become outward and their size increases with voltage. Note the strong distortion produced by these components on the time course of I_{Na} at + 40 mV. Below + 2 mV, the contribution of the TTX-insensitive component to the total current was negligible (not shown). Holding potential: − 80 mV. *Out:* 120 Na, 7 Mg. *In:* 130 Cs

current components flowing through incompletely blocked K^+ and Ca^{2+} channels. As shown in Fig. 5, membrane currents were recorded at various potentials before (curve *a*) and after addition of 3 μM TTX (curve *b*, TTX-insensitive currents), and their difference (curve $a-b$) was taken as the proper time course of I_{Na} (see Meves 1978). From these records, we estimated three relevant parameters of the sodium system (inset in Fig. 6): 1) the peak Na conductance, g_{Na}; 2) the time to peak, t_p, as a measure of activation; and 3) the time constant of inactivation, τ_h, which was determined by fitting a single exponential to the falling phase of the current trace as shown in the inset of Fig. 6.

Indeed, in some cells, Na currents appeared to possess additional inactivating components. A slow and occasionally a nearly maintained component, similar to that described in rat muscle fibres (Patlak and Ortiz 1985), were observed. Their variability, however, did not allow an unambiguous determination of the slow inactivation kinetics. We also found that in their presence, fitting of inactivation with a single exponential was a reasonable simplification.

Figure 6 presents the values of g_{Na}, t_p and τ_h at potentials ranging from − 30 to + 40 mV. Similar to Na channels in nerves, g_{Na} was steeply voltage-dependent at low voltages, with a maximum slope at − 30 mV (5 mV for an *e*-fold change in g_{Na}), and reached a maximum at about + 10 mV. t_p and τ_h also showed the typical voltage-dependent behavior described for other Na currents. From − 30 to + 40 mV, t_p decreased monotonically; at − 20 mV, it nearly halved for a 10 mV potential change. τ_h decreased even faster; at − 30 mV, it decreased approximately fourfold for a 10 mV change in potential.

As in nerve fibres, Na currents in DRG cells inactivated in the millisecond range in a voltage-dependent manner (fast inactivation). This is illustrated in Fig. 7, left, where the non-inactivated fraction of Na currents (h_∞) measured after a conditioning prepulse of 50 to 100 ms duration is plotted for varied membrane potentials. At 12 °C the h_∞-curve was *S*-shaped and had maximum slope near its midpoint (− 40 mV; filled circles). Changing the temperature from 12 °C to 20 °C (semi-filled circles) increased the steepness of the curve and shifted the midpoint about 4 mV to the left. A change from 12 °C to 8 °C had the opposite effect.

Na currents in DRG cells were also sensitive to variations of the holding potential (ultra-slow inactivation; Chandler and Meves 1970b; Fox 1976), as illustrated in Fig. 7, right. As shown, the size of the current decreased with less negative holding potentials. At $E_h = -70$ mV, the amount of Na current available on step depolarization to + 10 mV was 75% of that at − 100 mV. At − 60 mV, this value fell to 35% and to less than 10% at − 50 mV.

Effects of pronase and NBA on Na inactivation

As with the squid axon (Armstrong et al. 1973; Oxford et al. 1978), internal application of the enzyme pronase (1 mg/ml) or N-bromoacetamide (NBA, 0.4 mM) partially removed the fast Na inactivation of DRG cells (Fig. 8). Pronase (or NBA) produced a progressive increase of the maintained level of the current at long times, suggesting that after enzymatic treatment a fraction of channels could no longer be inactivated. The action of pronase in DRG cells was similar to that in squid

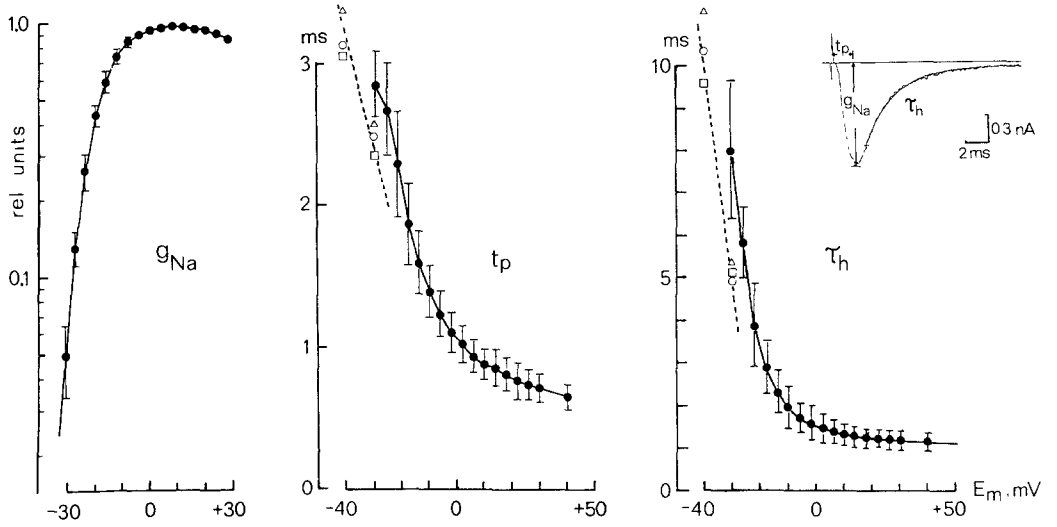

Fig. 6. Normalized peak amplitude (g_{Na}), time to peak (t_p), and inactivation time constant (τ_h) of Na conductance versus voltage. g_{Na} was calculated from I_{Na} records corrected for TTX-insensitive currents using the equation: $g_{Na}=I_{Na}(E-E_{Na})$. The inset on the top (right) of the figure shows how the three parameters g_{Na}, t_p, and τ_h were determined. τ_h was estimated by best fitting the decaying part of I_{Na} with a single exponential function. The fitting started at the time when g_{Na} was 80% of its peak value (cross in the inset) and ended after 7 ms. The current trace shown in the figure was received at − 18 mV and had $\tau_h = 1.69$ ms. *Dots* are values averaged over four cells. *Bars* are standard errors. The other symbols are data values of t_p^* and τ_h^* derived from the time course of the current averages of single Na channel recordings shown in Fig. 9. Holding potential: − 80 mV. *Out:* 120 Na, 7 Mg. *In:* 130 Cs

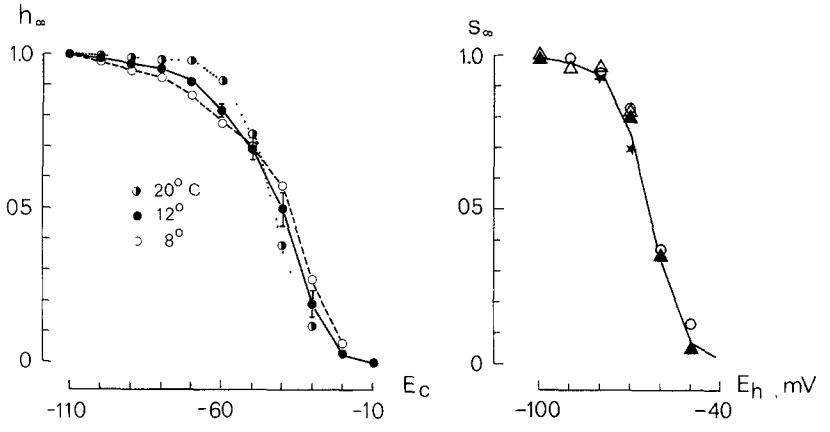

Fig. 7. *Left:* Voltage dependence of steady state Na inactivation (h_∞) at various temperatures. The peak I_{Na} during a test pulse to 0 mV was measured following conditioning prepulse (E_c) to various potentials, and plotted normalized to the value at − 110 mV. The conditioning prepulse lasted 50 ms at 12° and 20 °C and 100 ms at 8 °C. Dots are averages over four cells. Bars on filled circles (12 °C) are standard errors. The standard errors are similar at 8° *(circles)* and 20 °C *(semifilled circles)*. Holding potential: − 70 mV. *Right:* Effect of holding on I_{Na} (ultraslow inactivation). Cells were maintained for 120 s at various holding potentials, E_h, after which a 7 ms step pulse to + 10 mV was delivered. The value of peak I_{Na} measured during the test pulse was normalized to that at − 100 mV and plotted vs. holding potential. An interval of 120 s was found sufficiently long for s_∞ to reach a steady state value. Symbols represent data from different cells. *Out:* 120 Na, 7 Mg. *In:* 130 Cs

axons but inactivation removal was slower and less complete, probably because of the slow and irreversible dialysis of the cells. In addition, the peak amplitude of I_{Na} became strongly depressed (see figure legend), and leakage currents increased progressively until they masked the Na component within 5 to 10 min. Interestingly, in four cells high internal pH (9.2) was also found to remove Na inactivation (not shown). The action was similar to that in squid axons (Brodwick and Eaton 1978; Carbone et al. 1981), but accompanied by strong increases of leakage currents which prevented a quantitative study.

Singel Na channel recording

As in other preparations (Fenwick et al. 1982; Nagy et al. 1983; Cachelin et al. 1983; Horn et al. 1984;

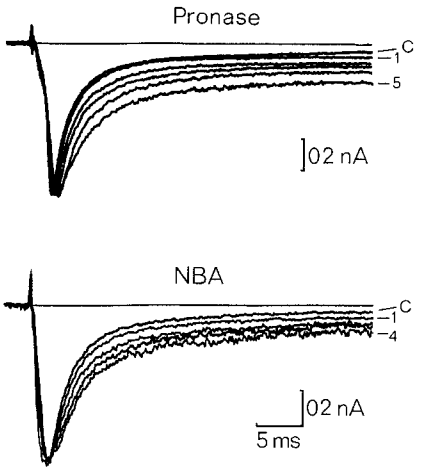

Fig. 8. Removal of Na inactivation by pronase and NBA. *Top:* Normalized sodium currents associated with step depolarizations to − 10 mV during the action of pronase (1 mg/ml). Trace *C* was recorded before the action of the enzyme began. The other traces (1−5) were recorded at intervals of 20 s. Note the increasing level of maintained current during pronase action. These traces are also noisier than the control. This is because they are multiplied by a scaling factor which increased from 1.1 (trace 1) to 2.1 (trace 5) to account for the peak amplitude depression observed during pronase treatment. *Bottom:* Effects of 0.4 m*M* NBA on normalized Na currents. Traces 1 and 4 were multiplied by factor of 1.1 and 2.7, respectively. Same conditions as above. Holding potential: − 70 mV. *Out:* 120 Na, 7 Mg. *In:* 130 Cs

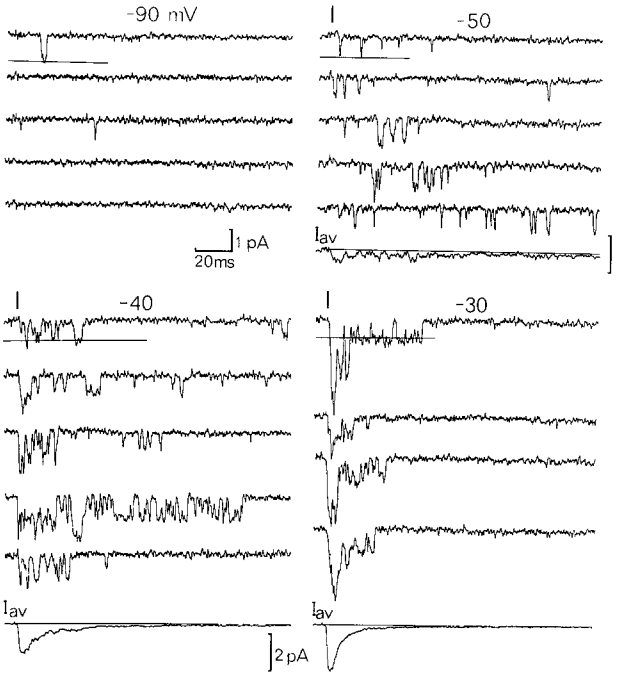

Fig. 9. Single Na channel currents in an outside-out patch recorded at the potential indicated. Horizontal lines in the first recording represent the detection level for opening. Bars indicate the onset of the depolarizing voltage steps. The bottom trace (I_{av}) at − 50, − 40 and − 30 mV is the average calculated from 48, 118 and 131 current samples, respectively. The holding potential was − 90 mV. In this patch, channel activity lasted about 40 min and showed no appreciable signs of rundown. Addition of TTX (3 μ*M*) at the end of the experiment resulted in a complete block of channel currents. Traces were corrected for leakage and capacitive currents as described in the Methods. The patch apparently contained 7−8 channels as estimated from the maximum number of simultaneous openings in response to large depolarizations. The vertical bar near I_{av} at − 50 mV corresponds to 0.5 pA. Filter bandwidth: 1 kHz. *Out:* 120 Na, 7 Mg. *In:* 130 Cs

Fernandez et al. 1984), unitary Na channel events were resolved in outside-out membrane patches, using Ca- and K-free media and pipettes containing Cs and TEA (see Table 1). Figure 9 shows examples of single channel recordings at various potentials. At − 90 mV, channels opened occasionally or not at all during samples of 160 ms duration. With steps higher than − 50 mV, channel openings became more frequent. The probability of occurrence was higher shortly after the onset of the step depolarization than at later times, indicating time-dependent inactivation. Inactivation developed faster and the average time to first opening was shortened with increasing voltages. At − 50 mV, first openings occurred as late as 25 ms after the onset of the step (fourth trace from the top), and channel activity lasted until the end of the pulse (bottom trace). At − 30 mV, multiple channel openings occurred immediately after the beginning of a pulse and activity ceased within 50 ms. Single channel activity could be fully blocked by adding 3 μ*M* TTX to the external bath.

The time course of the sample averages (I_{av}) strongly resembled that of I_{Na} recorded in whole cell conditions. The time to peak, t_p^*, was shortened and the time constant of inactivation, τ_h^*, decreased with

Table 1. Solutions [m*M*][a]

External	NaCl	KCl	$CaCl_2$	$MgCl_2$	Chol. Cl	Na-HEPES [pH 7.3]
5 Ca, 0 K	120	–	5	2	–	10
1 Ca, 3 K	120	3	1	2	–	10
2 Ca, 0 K	120	–	2	2	–	10
0 Ca, 7 Mg	120	–	–	7	–	10
120 Chol.	–	–	5	2	120	10

Internal	NaCl	KCl	$CaCl_2$	EGTA	CsCl	TEACl	Na-Hepes [pH 7.3]
120 K	3	120	1	5	–	–	10
120 Cs	10	–	1	5	120	20	10
130 Cs	–	–	0.25	5	130	20	10

[a] The osmolarity of all solutions was adjusted to 300 mosmol. with glucose

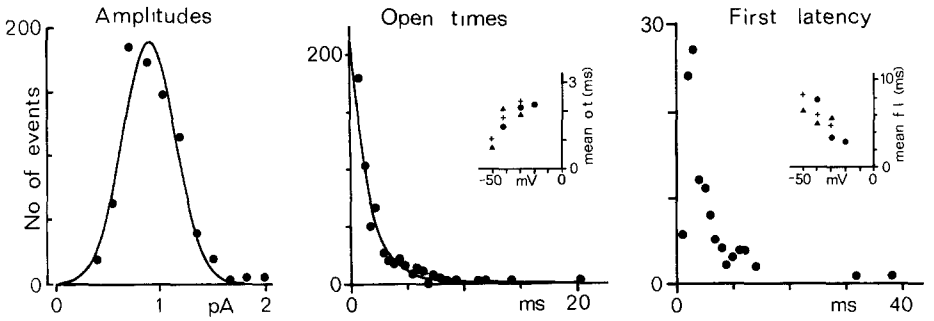

Fig. 10. Statistical analysis of single Na channels events. *Left:* Example of amplitude histogram obtained from idealized channel events at − 40 mV. The solid line is a Gaussian curve fitted to the data. Mean and standard deviation were 0.9 and 0.25 pA, respectively. Under similar conditions, mean amplitudes were 1.02 and 0.79 pA at − 50 and − 30 mV, respectively. *Middle:* Open time distribution at − 40 mV. The solid line is a best fitting exponential with a time constant of 1.8 ms. Under the same conditions, mean open times were 1.2 and 2.3 ms at − 50 and − 30 mV, respectively. *Inset:* Mean open times (o.t.) as a function of voltage. Different symbols indicate different cells. *Right:* Latency-to-first-opening histogram at − 40 mV. The mean first latency (f.l.) for this experiment was 6 ms. Under the same conditions, f.l. was 8.2 and 5.4 ms at − 50 and − 30 mV, respectively. *Inset:* Mean first latency versus voltage. Data were pooled from three patches which contained an apparently similar number of channels (7 to 8). Although histograms were not corrected for the number of channels, this condition would allow to combine values of mean latencies derived from different patches (Patlak and Horn 1982). Ionic conditions were similar to those of Fig. 9

increasing voltage. Changing the potential from − 50 to − 30 mV, t_p^* decreased from 5 to 2.5 ms and τ_h^* fell from 32 to 4.8 ms. These values agree well with those of t_p and τ_h estimates for I_{Na}, if allowance is made for a voltage shift of − 10 to − 20 mV (see open symbols in Fig. 6). This is similar to previous observations on the Na channel of other preparations using the same technique (Fenwick et al. 1982; Nagy et al. 1983; Fernandez et al. 1984).

Analysis of single channel recording

Single channel events were analyzed by converting current traces into idealized records as described in Methods. The amplitude, open time, and first latency of the idealized events were computed and the corresponding histograms were constructed (Lux and Brown 1984). The amplitude distribution of the events could be fitted by a Gaussian curve (Fig. 10, left). At − 50 mV the mean of the amplitude histogram was 1.02 pA, which decreased to 0.79 pA at − 30 mV, giving a slope conductance (γ) of 11.5 pS in this range of potentials. The average γ of five patches was: 10.8 ± 2.3 pS (mean ± SD). The open time distributions were fitted well with single exponential functions (Fig. 10, middle). Mean open times were calculated at different membrane depolarizations and plotted vs. voltage (see inset). As shown, the mean open time increased nearly twofold for a change in voltage from − 50 to − 40 mV, and settled to a constant value at higher depolarizations. For this patch, which probably contained 7 to 8 channels, latencies to first-opening histograms showed a maximum at about 3 ms after the onset of a depolarization to − 40 mV, and decreased rapidly at later times (Fig. 10, right). At depolarized voltages, the time to peak decreased and the histograms were more compressed. Mean latencies to first event were evaluated and plotted as a function of voltage (see inset). As shown, the maximum of the distribution decreased monotonically with depolarization from − 50 to − 20 mV. This agrees qualitatively with previous measurements on other Na channels (Horn et al. 1984).

Effects of pronase

The presence of pronase (0.1 mg/ml) at the inner side of an outside-out patch led to a drastic prolongation of the single channel activity (Fig. 11). At potentials between − 50 and − 40 mV, openings occurred in rapid succession and showed signs of bursting activity. In samples of 250 ms, bursting activity could be continuous (traces 4 and 8 in Fig. 11) or interrupted by long lasting closures (traces 1 and 6). At − 50 mV, there were double openings which appeared to have the same probability of occurrence at the beginning as well as at the end of the pulse (traces 2 and 4), indicating a weaker time-dependent inactivation than in control patches. This was also evident from the time course of the sample averages (bottom traces in the figure), which showed incomplete inactivation for the entire pulse duration.

Pronase did not appear to affect the mean amplitude of the events. In five patches γ varied from 9.5 and 12.3 pS and the mean open time increased by a factor of about 3 in the potential range − 50 to − 40 mV. In two patches, the lifetimes of the channel increased by a factor of 5 to 10 at stronger depolar-

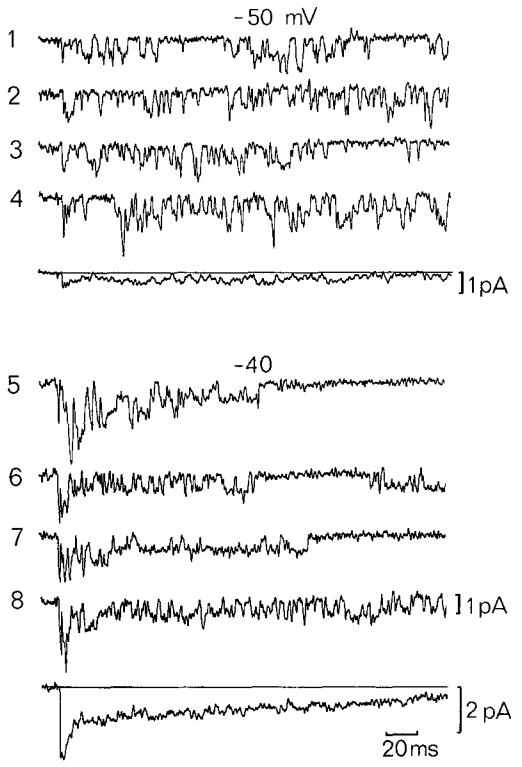

Fig. 11. Single Na channel recording in pronase-treated outside-out patches, at the potential indicated. Ionic conditions were similar to those of Fig. 9, except that the solution-pipette contained 0.1 mg/ml Pronase. The holding potential was − 100 mV. The last trace at each potential is the average of 15 (− 50 mV) and 29 (− 40 mV) samples. Note the prolonged intervals of channel activity in the presence of the enzyme compared to that of untreated patches in Fig. 9. Mean open times were 3.1 and 6.4 ms at − 50 and − 40 mV, respectively. Mean first latencies were 4 and 2 ms at − 50 and − 40 ms, i.e. slightly shorter than those in untreated patches. This, however, could be an effect of the more negative holding potential which was also observed in three other patches. There were no more than 4 active channels in the patch as shown by the maximum number of simultaneous openings at large depolarizations

izations (− 30 to − 10 mV, not shown). This agrees with recent findings by Horn et al. (1984), on NBA treated outside-out patches of GH3 pituitary cells, but not with observations on excised patches of rat myoballs (Patlak and Horn 1982).

Discussion

This paper shows that whole cell and single-channel Na currents in primary cultures of dissociated chick sensory neurons can be studied with sufficient accuracy after pharmacological elimination of other membrane currents. Following usual separation procedures, Na currents in chick DRG appear to have properties close to those of peripheral nerve fibres (Armstrong 1981; French and Horn 1983) and neuronal cell lines (Moolenaar and Spector 1978): *i)* activation and inactivation are time- and voltage-dependent; *ii)* currents are fully blocked by TTX; and *iii)* internal pronase and NBA make inactivation incomplete.

Comparison with other Na currents

As shown in Table 2, peak Na current density, I_p, in chick DRG is comparable to that of mouse neuroblastoma (Moolenaar and Spector 1978), bovine chromaffin cells (Fenwick et al. 1982), and GH3 pituitary cells (Dubinsky and Oxford 1984; Matteson and Armstrong 1984), and about one to two orders of magnitude smaller than that in squid axon (Hodgkin and Huxley 1952a) and frog node (Dodge and Frankenhäuser 1959). A γ of 11 ± 2 pS gives a density of Na channels in chick DRG of 1 to 5 per μm^2. This estimate increases to 2–20 channels per μm^2 if one accounts for the 50 to 75% loss of Na channels which are already inactivated at the time

Table 2. Peak Na current density in excitable cells

Cell	I_p [mA · cm^{-2}]	E_t[a] [mV]	Temp. [°C]	Authors
Squid axon	1.3	−10	5	Hodgkin and Huxley (1952)
Frog node	13	−20	20	Dodge and Frankenhäuser (1959)
Snail neuron	0.5[b]	−6	13.5	Adams and Gage (1979)
Mouse neuroblastoma	0.4	−10	20	Moolenar and Spector (1978)
Bovine chromaffine	0.06	+10	20	Fenwick et al. (1982)
Rat pituitary GH3	0.1	+12	22	Dubinsky and Oxford (1984)
Rat pituitary GH3	0.2	0	22	Matteson and Armstrong (1984)
Rat DRG	0.07[b]	−25	20	Kostyuk et al. (1981)
Guinea pig DRG	2.5	0	20	Kameyama (1983)
Chick DRG	0.5	+10	25	Dunlap and Fischbach (1981)
Chick DRG	0.2	−10	12	This work

[a] E_t is the membrane potential at which the reported values of I_p have been measured
[b] These values were not explicitly indicated in the paper. They were computed by us, taking representative values of I_p and dividing them by the reported average area of the cells

Table 3. t_p and τ_h in various excitable cells

Cell	t_p [ms]	τ_h [ms]	τ_h/t_p	E_t [mV]	Temp. [°C]	Authors
Squid axon	0.5	1.5	3	0	6	Hodgkin and Huxley (1952)
Myxicola axon	0.6	1.5	2.5	−3	5	Goldman and Schauf (1973)
Crayfish axon	0.35	0.45	1.3	0	8	Swenson (1980)
Aplysia neuron	5	18	3.6	−6	13.5	Adams and Gage (1979)
Frog node	0.15	0.5	3.3	0	20	Frankenhäuser (1963)
Rabbit node	0.7	0.9	1.3	−35	14	Chiu et al. (1978)
Mouse neuroblastoma	0.5	0.5	1	−8	20	Moolenar and Spector (1978)
Chick DRG	1.1	1.5	1.4	0	12	This work
Bovine chromaffine	0.7	1.2	1.7	0	20	Fenwick et al. (1982)
Rat pituitary GH3	1.5	2.2	1.5	0	20	Dubinsky and Oxford (1984)
Rat pituitary GH3	0.7	1.1	1.6	+20	20	Matteson and Armstrong (1984)

of peak I_{Na} (Matteson and Armstrong 1984). This channel density is one to two orders of magnitude smaller than that in peripheral nerve fibres (Conti et al. 1975; Conti et al. 1976), but is close to that of other cell bodies (Sigworth and Neher 1980; Fenwick et al. 1982; Cachelin et al. 1983).

The time course of inactivation is fast with respect to activation, as revealed by the low value of the ratio τ_h/t_p (see Table 3). For all the cell cultures examined, including chick DRG, τ_h/t_p ranges between 1 and 1.7. This value is comparable to that of crayfish axon (Swenson 1980) and rabbit node (Chiu et al. 1978), but is about a factor of 2 to 3 smaller than in squid axon (Hodgkin and Huxley 1952 b), myxicola axon (Goldman and Schauf 1973), and frog node (Frankenhäuser 1963). We do not have a clear explantation for this but it is suggestive to speculate that, at least in the case of sensory neurons, a fast Na inactivation process would result in a more efficient usage of Na channels at the cell body. It may be that in DRG cells the action potential functions primarily to regulate the influx of calcium ions required for the release of endogenous neuropeptides (Otsuka and Konishi 1976; Mudge et al. 1979). In this case, a faster Na inactivation would speed up the early repolarization phase of the soma spike, allowing the membrane potential in shorter time to reach levels for which Ca^{2+} entry is maximal (0, +10 mV), with consequent increases of the intracellular Ca^{2+}.

Na currents in DRG cells can be blocked by TTX and modified internally by pronase and NBA, as shown in Figs. 3 and 8. At concentrations of 3 μM, TTX completely abolished I_{Na}, but complete block could also be achieved with a ten times lower concentration. These results indicate that for the Na channel of chick DRG the dissociation constant of the toxin-receptor complex, K_D, may be similar to that of squid axon (Cuervo and Adelman, 1973) and frog node (Schwarz et al. 1973), in which full block of I_{Na} occurs with TTX concentrations above 0.3 μM. As in the case of squid axon the action of pronase and NBA is to irreversibly remove Na current inactivation with little effect on the rate of activation and inactivation (Armstrong et al. 1973; Oxford et al. 1978).

Unitary Na currents

The single channel conductance (11 pS), mean open time (1−3 ms), and range of voltage activation (− 50, − 20 mV) of Na channels in chick DRG are close to those reported for rat myoballs (Sigworth and Neher, 1980; Patlak and Horn 1982), chromaffin cells (Fenwick et al. 1982), mouse neuroblastoma (Nagy et al. 1983), GH_3 cells (Horn et al. 1984) and rat ventricular myocytes (Kunze et al. 1985). Inactivation of channel activity (as indicated by the time course of current averages in Fig. 9) is fast, voltage-dependent and strongly affected by internal pronase (Fig. 11).

The population of Na channels in DRG cells appears rather homogeneous as proved by the amplitudes and open time distributions (Fig. 10). This is similar to other cell preparations (see French and Horn 1983) but differs from mouse neuroblastoma (Nagy et al. 1983) in which Na channels were suggested to possess two open states with distinct amplitude and mean open time. Indeed, a second population of Na channels of lower amplitude and shorter lifetime could have been missed in our analysis due to both the high detecting level for channel openings (which was 2/3 of the average amplitude of the events) and an effective minimal detectable duration of 140 μs for channel opening. However, the requirements for identifying openings against background noise precluded the search for a distinct population of channels with opening amplitudes below the detection level employed.

The mean open time of Na channels in chick DRG varies between 1 and 3 ms and is weakly voltage-dependent in the potential range of − 50 to − 20 mV. This is close to the data from outside-out patches of other preparations (Fenwick et al. 1982; Nagy et al. 1983; Cachelin et al. 1983; Horn et al. 1984), but is a factor 2 to 6 larger than that reported by Aldrich et al. (1983) for cell-attached patches of mouse neuroblastoma cells.

Kinetic models

An interesting finding of our study is that at low depolarizations (− 50 to − 40 mV) in pronase-treated patches, openings of Na channels occur in bursts and their lifetime is prolonged by only a factor of three. This is similar to NBA treated patches of GH_3 cells (Horn et al. 1984), reinforcing the view that at low membrane potentials the lifetime of channel openings is controlled by both the rate of inactivation and channel closing. Our data can be explained by following similar arguments.

Assuming that the closed (C), open (O) and inactivated (I) state of the Na channel are related as indicated below (see Aldrich et al. 1983; Horn and Vandenberg 1984):

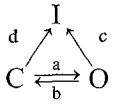

the lifetime of the open state (τ_0) is determined by the ratio $1/(b+c)$. If pronase acts on Na channels mainly by removing the transition rate c and d (Armstrong et al., 1973), then in pronase-treated patches where all channels can no longer inactivate, $\tau_0 = 1/b$ (Horn et al. 1984). In our case, pronase appears to remove inactivation only in half of the channels in the patch (see the time course of the average current at − 40 mV in Fig. 11), making an analytical determination of τ_0 more complicated. On the other hand, channel activity in pronase-treated patches is preserved well after the full development of inactivation ($\tau_h^* \simeq 10$ ms), suggesting that an estimate of τ_0 during depolarizing pulses 20 to 25 times longer than τ_h^*, as shown in Fig. 11, would result in an accurate determination of the open lifetime of those channels which are no longer able to inactivate.

Following these arguments, the threefold increase of τ_0 observed in pronase-treated patches would imply that the constant b is only two times smaller than c, and of the order of 0.15 ms^{-1} at − 40 mV. In other words, in control patches, an open channel has a probability of closing which is comparable to that of inactivating (Vandenberg and Horn 1984). That is to say, open Na channels in DRG cells can close several times before entering an inactivated (absorbing) state. This is different from that proposed by Aldrich et al. (1983), for the Na channel in the cell-attached configuration of mammalian nerve cells; namely, that channels primarily open only once per depolarization and close to an inactivated state without reopening. In our case, this seems to hold true only at larger membrane depolarizations (− 20 to + 10 mV) where mean lifetimes in the presence of pronase are 10 times larger than in the control. A confirmation of this, however, must wait for further experimental work.

Acknowledgements. We are grateful to Prof. A. M. Brown for stimulating discussions, to Mrs. I. Kiss and H. Tyrlas for technical assistance.

This work was supported in part by a grant from the Deutsche Forschungsgemeinschaft (SFB 1138/A1).

References

Adams DJ, Gage PW (1979) Characteristics of sodium and calcium conductance changes produced by membrane depolarization in an *Aplysia* neurone. J Physiol (Lond) 289:143–161

Aldrich RW, Corey DP, Stevens CF (1983) A reinterpretation of mammalian sodium channel gating based on single channel recording. Nature 306:436–441

Almers W, McCleskey EW (1984) Non selective conductance in calcium channels of frog muscle: calcium selectivity in a single-file pore. J Physiol (Lond) 353:585–628

Armstrong CM (1981) Sodium channels gating currents. Physiol Rev 61:644–683

Armstrong CM, Bezanilla F, Rojas E (1973) Destruction of sodium conductance inactivation in squid axons perfused with pronase. J Gen Physiol 62:375–391

Baccaglini PI (1978) Action potentials of embryonic dorsal root ganglion neurons in *Xenopus* tadpoles. J Physiol (Lond) 283:585–604

Barde YA, Edgar D, Thoenen H (1980) Sensory neurons in culture: changing requirements for survival factors during embryonic development. Proc Natl Acad Sci USA 77:1199–1203

Brodwick MS, Eaton DC (1978) Sodium channel inactivation in squid axon is removed by high internal pH or tyroxine-specific reagents. Science 200:1494–1496

Carbone E, Lux HD (1984a) A low voltage-activated calcium conductance in embryonic chick sensory neurons. Biophys J 46:413–418

Carbone E, Lux HD (1984b) A low voltage-activated, fully inactivating Ca channel in vertebrate sensory neurons. Nature 310:501–502

Carbone E, Lux HD (1984c) Single Na and Ca channels in vertebrate sensory neurons. Int. Congr. Biophys Abstr (Bristol) 1:272

Carbone E, Testa PL, Wanke E (1981) Intracellular pH and ionic channels in the *Loligo vulgaris* giant axon. Biophys J 35:393–413

Chachelin AB, De Peyer JE, Kokubun S, Reuter H (1983) Sodium channels in cultured cardiac cells. J Physiol (Lond) 340:389–401

Chandler WK, Meves H (1970a) Evidence for two types of sodium conductance in axons perfused with sodium fluoride solutions. J Physiol (Lond) 211:653–678

Chandler WK, Meves H (1970b) Slow changes in membrane permeability and longlasting action potentials in axons perfused with fluoride solutions. J Physiol (Lond) 211:707–728

Chiu SY, Ritchie JM, Rogart RB, Stagg D (1979) A quantitative description of membrane currents in rabbit myelinated nerve. J Physiol (Lond) 292:149–166

Conti F, DeFelice LJ, Wanke E (1975) Potassium and sodium ion current noise in the membrane of the squid giant axon. J Physiol. (Lond) 248:45–82

Conti F, Hille B, Neumcke B, Nonner W, Stämpfli R (1976) Measurement of the conductance of the sodium channel from current fluctuations at the node of Ranvier. J Physiol (Lond) 262:699–727

Cuervo LA, Adelman WJ (1970) Equilibrium and kinetic properties of the interaction between tetrodotoxin and the excitable membrane of the squid giant axon. J Gen Physiol 55:309–335

Dichter MA, Fischbach GD (1977) The action potential of chick dorsal root ganglion neurones maintained in cell culture. J Physiol (Lond) 267:281–298

Dodge FA, Frankenhäuser B (1959) Sodium currents in the myelinated nerve fibre of *Xenopus Laevis* investigated with the voltage clamp technique. J Physiol (Lond) 148:188–200

Dubinsky JM, Oxford GS (1984) Ionic currents in two strains of rat anterior pituitary tumor cells. J Gen Physiol 83:309–339

Dunlap K, Fischbach GD (1981) Neurotransmitters decrease the calcium conductance activated by depolarization of embryonic chick sensory neurons. J Physiol (Lond) 317:519–535

Fenwick EM, Marty A, Neher E (1982) Sodium and calcium channels in bovine chromaffin cells. J Physiol (Lond) 331:599–635

Fernandez JM, Fox AP, Krasne S (1984) Membrane patches and whole cell membranes: a comparison of electrical properties in rat clonal pituitary (GH_3) cells. J Physiol (Lond) 356:565–585

Fox JM (1976) Ultra-slow inactivation of the ionic currents through the membrane of the myelinated nerve. Biochim Biophys Acta 426:245–257

Frankenhäuser B (1963) Inactivation of the sodium-carrying mechanism in myelinated nerve fibres of *Xenopus Laevis.* J Physiol (Lond) 169:445–451

French RJ, Horn R (1983) Sodium channel gating: Models, Mimics and Modifiers. Annu Rev Biophys Bioeng 12: 319–356

Goldman L, Schauf CL (1973) Quantitative description of sodium and potassium currents and computed action potentials in *Myxicola* giant axons. J Gen Physiol 61:361–384

Hamill OP, Marty A, Neher E, Sakmann B, Sigworth FJ (1981) Improved patch-clamp techniques for high-resolution current recording from cells and cell-free membrane patches. Pflügers Arch 391:85–100

Hess P, Tsien RW (1984) Mechanisms of ion permeation through calcium channels. Nature (Lond) 309:453–456

Hodgkin AL, Huxley AF (1952a) The dual effect of membrane potential on sodium conductance in the giant axon of Loligo. J Physiol (Lond) 116:497–506

Hodgkin AL, Huxley AF (1952b) A quantitative description of membrane current and its application to conduction and excitation in nerve. J Physiol (Lond) 117:500–544

Horn R, Lange K (1983) Estimating kinetics constants from single channel data. Biophys J 43:207–223

Horn R, Vandenberg CA (1984) Statistical properties of single sodium channels. J Gen Physiol 84:505–534

Horn R, Vandenberg CA, Lange K (1984) Statistical analysis of single Na channels. Effects of N-Bromoacetamide. Biophys J 45:323–335

Ishizuka S, Hattori K, Akaike (1984) Separation of ionic currents in the somatic membrane of frog sensory neurons. J Membr Biol 78:19–28

Kameyama M (1983) Ionic currents in cultured dorsal root ganglion cells from adult guinea pigs. J Membr Biol 72:195–203

Kostyuk PG, Veselovsky NS, Tsyndrenko AY (1981) Ionic currents in the somatic membrane of rat dorsal root ganglion neurons. I. Sodium currents. Neuroscience 6:2423–2430

Kostyuk PG, Veselovsky NS, Fedulova SA (1981) Ionic currents in the somatic membrane of rat dorsal root ganglion neurons. II. Calcium currents. Neuroscience 6:2431–2437

Kunze DL, Lacerda AE, Wilson DL, Brown AM (1985) Reopening, waiting and inactivating properties of single Na channels. J Gen Physiol (in press)

Lux HD, Brown AM (1984) Patch and whole cell calcium currents recorded simultaneously in snail neurons. J Gen Physiol 83:727–750

Matteson DR, Armstrong CM (1984) Na and Ca channels in a transformed line of anterior pituitary cells. J Gen Physiol 83:371–394

Meves H (1978) Inactivation of the sodium permeability in squid giant fibres. Prog Biophys Mol Biol 33:207–230

Moolenaar WH, Spector I (1978) Ionic currents in cultured mouse neuroblastoma cells under voltage-clamp conditions. J Physiol (Lond) 278:265–286

Mudge AW, Leeman SE, Fischbach GD (1979) Enkephalin inhibits release of substance *P* from sensory neurons in culture and decreases action potential duration. Proc Natl Acad Sci USA 76:526–530

Nagy K, Kiss T, Hof D (1983) Single Na channels in mouse neuroblastoma cell membrane. Indications for two open states. Pflügers Arch 399:302–308

Otsuka M, Konishi S (1976) Substance *P* and excitatory transmitter of primary sensory neurons. Cold Spring Harbor Symp Quant Biol 40:135–143

Oxford GS, Wu CH, Narahashi T (1978) Removal of sodium channel inactivation in squid giant axons by N-bromoacetamide. J Gen Physiol 71:227–247

Patlak J, Horn R (1982) Effect of N-bromoacetamide on single sodium channel currents in excised membrane patches. J Gen Physiol 79:331–351

Patlak JB, Ortiz M (1985) Slow currents through single sodium channels of the adult rat heart. J Gen Physiol 86:89–104

Schwarz IR, Ulbricht W, Wagner HH (1973) The rate of action of tetrodotoxin on myelinated nerve fibres of *Xenopus Laevis* and *Rana Esculenta.* J Physiol (Lond) 233:167–194

Sigworth FJ, Neher E (1980) Single Na^+ channel currents observed in cultured rat muscle cells. Nature (Lond) 287:447–449

Swenson RP (1980) Gating charge immobilization and sodium current inactivation in internally perfused crayfish giant axons. Nature (Lond) 287:644–645

Vandenberg CA, Horn R (1984) Inactivation viewed through single sodium channels. J Gen Physiol 84:535–564